HYDROGEN, FUEL CELL &
ENERGY STORAGE
ECSI IHFCA IROST

Boosting Mg-Air Battery Efficiency with Polyaniline-Coated Anodes

Fatemeh Parvinzadeh[a] | **Mehdi Kheirmand**[a,b,*] | **Parisa Akbarian**[a]

[a] Hydrogen and Fuel Cell Research Laboratory, Chemistry Department, Yasouj University, Yasouj, Iran
[b] Chemistry Department, School of Basic Sciences, Yasouj University, PO Box 75918-74934, Yasouj, Iran
[*] Corresponding author, Email: kheirmand@yu.ac.ir

Article Information

Article Type
RESEARCH ARTICLE

Article History
RECEIVED: *24 Nov 2025*
REVISED: *10 Feb 2026*
ACCEPTED: *02 Mar 2026*

Keywords

Mg-Air battery
Anode surface modification
PANI
Self-corrosion
Mg anode

Abstract

Despite the abundance and high density of Mg metal as an anode, the limited development of Mg-air batteries is primarily due to the surface reactions of the Mg anode in water-based electrolytes. A reliable strategy to improve metal anode efficiency is to prevent anode surface reactions by designing and applying suitable protective coatings. In this study, a polyaniline (PANI) polymer coating was designed and synthesized to modify the surface of Mg anodes. The primary scope of this research is to examine the effect of coating on the Mg anode surface and its ability to control surface reactions, including corrosion. Electrochemical analyses confirm the optimal efficiency of the PANI coating in inhibiting the corrosion of the surfaces of Magnesium, as evidenced by comparisons between uncoated and PANI-coated samples. As a result, Mg with PANI coating has a smaller corrosion current and a larger corrosion potential (5.06×10^{-5} A/cm^2, 1.01 V) than uncoated Mg (6.3×10^{-4} A/cm^2, 1.49 V), respectively. Because of its chemical durability and good electrochemical behavior, PANI can overcome the limitations of using Mg anodes as a protective surface coating, improving the efficiency of Mg-air batteries and developing new technologies.

Cite this article: Parvinzadeh, F., Kheirmand, M., Akbarian, P. (2026). Boosting Mg-Air Battery Efficiency with Polyaniline-Coated Anodes. DOI: 10.22104/hfe.2025.7564.1353

Publisher: Iranian Research Organization for Science and Technology (IROST)
DOI: 10.22104/hfe.2025.7564.1353

1 Introduction

The development of clean, eco-friendly power storage and conversion technologies is essential. Among the leading energy technologies, fuel cells and metal-air batteries are notable for their environmental compatibility, high efficiency, and sustainable design. Rechargeable metal-air batteries can significantly alleviate the energy crisis and environmental pollution. As versatile energy storage devices utilizing electrochemical processes, these batteries have the potential to create a carbon-free and sustainable future [1, 2]. Metal-air batteries are distinguished by their ability to provide continuous energy, high energy density, and cost-effective design, making them effective for electrochemical energy storage and conversion. Furthermore, they offer advantages such as compact size, low weight, enhanced safety, and excellent environmental compatibility [3,4]. In metal-air batteries, the porous air electrode facilitates oxygen diffusion and acts as a catalyst substrate [5]. Rechargeable magnesium-air batteries are particularly significant to enable energy storage as a result of their lightweight, low toxicity, and high safety. Mg-air batteries can be reused by substituting the depleted magnesium anode and electrolyte with new ones. A 3.5% NaCl electrolyte is suitable for the Mg-air battery electrolyte. The overall electrochemical reactions in Mg-air batteries are as follows: Anode reaction [6]:

$$\mathrm{Mg} \longrightarrow \mathrm{Mg}^{2+} + 2\,\mathrm{e}^- \qquad (1)$$

Cathode reaction (in neutral/alkaline media):

$$\mathrm{O}_2 + 2\,\mathrm{H}_2\mathrm{O} + 4\,\mathrm{e}^- \longrightarrow 4\,\mathrm{OH}^- \qquad (2)$$

Magnesium-air batteries face efficiency challenges due to hydrogen release and the accumulation of an inactive $Mg(OH)_2$ layer, leading to corrosion and reduced performance [7–9]. To address these issues, researchers focus on improving magnesium's corrosion resistance through alloying and surface modification [10, 11]. Research efforts focus on improving battery efficiency through the use of Mg alloys, electrolyte additives, anti-corrosion coatings, and catalysts to enhance battery efficiency. High polarization is another critical problem, requiring electrode materials with low corrosion rates. Optimizing anode structure, increasing active sites, and improving cathode performance through hybrid catalysts and multilayer structures are key strategies [12–15]. Rapid anode corrosion limits the widespread application, but methods like alloying and protective coatings help mitigate this issue [16]. The development of physical barrier coatings and efficient electrocatalysts, including conductive polymers, is essential for enhancing Mg-air battery performance and energy conversion efficiency [17–21].

In the meantime, polyaniline (PANI) is utilized across various fields, encompassing microelectronics, corrosion-resistant coatings, sensors, and battery electrodes, owing to its versatile structure, stability under thermal and radiation conditions, affordability, simple synthesis, and conductivity. The unique electrical and optical properties of PANI have garnered significant attention. Among conductive polymers, PANI and polypyrrole are recognized as the most important. Their outstanding electrical performance, stability under environmental conditions, and cost-effective synthesis have made these compounds the focus of extensive research. PANI stands out due to its easy synthesis, inexpensive monomer, different oxidation states, good electrical conductivity, oxidation-reduction reversibility, and environmental stability. These attributes make PANI suitable for applications spanning multiple areas, such as sensors, electrochemical capacitors, and corrosion protection [22–31].

In metal-air batteries, the anode plays a significant role in defining the discharge performance and actual capacity, making the selection of an anode material a key factor. In recent decades, substantial research efforts have concentrated on Zn-air and Al-air batteries, whereas Mg-air batteries have been relatively overlooked. Studies on magnesium and its alloys as anode materials have progressed significantly. Methods such as alloying, heat treatment, and plastic deformation have been adopted to increase magnesium anode efficiency. A combined application of these techniques is fundamental for developing magnesium alloy anodes with improved discharge potential and minimized self-corrosion. Additionally, first-principles calculations offer valuable theoretical guidance and future projections [32].

Xue et al. proposed a superhydrophobic ODA/PDA/APT-Ce^{3+} (OPA-Ce^{3+}) coating with corrosion inhibition and self-healing properties by incorporating cerium nitrate (APT)-loaded attapulgite (APT) and polydopamine [33]. Additionally, Guo et al. reviewed synthetic methods of LDH coatings and LDH-based composite coatings on magnesium alloys, focusing on self-healing, biocompatibility, and self-cleaning properties [34].

This study investigates the use of magnesium as an anode in magnesium-air batteries and explores the enhancement of its electrochemical performance through a PANI coating. By applying a protective layer of PANI to pure magnesium, we aim to improve discharge activity, reduce self-corrosion, and increase overall efficiency. The effectiveness of this polymer coating as an anode electrode material was analyzed to assess its potential benefits for battery performance.

2 Experimental

2.1 Materials and methods

All chemicals used in this research project were obtained from Merck, Sigma-Aldrich, Cam-Lab, and Cabot companies and were used without additional purification. Samples were analyzed using a MIRA3 Field Emission Scanning Electron Microscope (FESEM) for surface morphology and an Oxford Instruments Energy Dispersive X-ray Spectroscopy (EDX) system for elemental composition. Structural analysis was performed using a Pert Pro X-ray Diffraction (XRD) system. Additionally, Inductively Coupled Plasma Optical Emission Spectroscopy (ICP-OES) was employed to accurately determine trace element concentrations with high precision.

2.2 Synthesis of PANI

The synthesis of PANI coating begins with the purification of 100 mL of Merck aniline through vacuum distillation at 125 °C for 2 hours, using a vacuum pump to reduce pressure, while maintaining the vacuum at 120 °C and adding calcareous stone to improve the distillation process. After purification, 0.5 mL of distilled aniline is mixed with 50 mL of 1 M HCl, stirred for 15 minutes, while separately dissolving 1.45 g of $(NH_4)_2S_2O_8$ in another 50 mL of 1 M HCl, also stirred for 15 min. The aniline solution is then placed in an ice bath at 0°C, followed by the slow addition of the oxidizing agent solution drop by drop over 30 minutes, leading to the formation of a green-colored solution, signifying successful polymerization. The resulting solution is filtered and washed with 100 mL of 0.3 M HCl, then left at room temperature for 24 hours. A dark green, sludgy precipitate forms, indicating the successful synthesis of polyaniline.

2.3 Preparation of Mg-PANI electrode

For the Mg anode coating, the anode surface is prepared by cleaning it with 2000-grit sandpaper, followed by ultrasonication in acetone for 20 min to remove contaminants. The coating mixture is then formed by combining the synthesized PANI with Nafion and acetylene black (0.007 g) and thoroughly stirring it for uniform consistency. The final coating is applied to the Mg surface via the spray method and allowed to dry in an oven at 80 °C for 2 hours, ensuring enhanced adhesion and stability for further testing.

2.4 Electrochemical measurements

A standard three-electrode system, connected to an EG&G potentiostat/galvanostat (PARSTAT 2273), was employed for all electrochemical experiments, with Pt and Ag/AgCl serving as the auxiliary and reference electrodes, respectively. Magnesium coated with as-synthesized PANI (surface area: $3\,\mathrm{cm}^2$) was used as the working electrode, and all measurements were carried out in a 3.5% NaCl electrolyte. To examine the electrochemical characteristics of the coating materials, methods including Tafel, Electrochemical Impedance Spectroscopy (EIS), and open circuit potential (OCP) at room temperature were employed. EIS measurements were conducted across a frequency range of 0.1 Hz to 100 kHz at an AC voltage of 10 mV. Before the electrochemical test, the surface of Mg was polished with 2000-grade SiC abrasive paper. Polarization Tafel curves were recorded with scanning potential from -0.5 V vs. saturated calomel electrode (SCE) in the anodic direction at 1 mV/s. The CP test was conducted for 600 sec at a current of 10 and 70 mA for evaluating the stability of the anode surface. The EIS was measured after immersing the tested samples in an electrolyte for 15 min at OCP. The frequency ranged from 0.1 Hz to 100 kHz, with an amplitude of 5 mV. A battery test system (battery tester-5CH) was employed to measure the discharge performance of Mg-air batteries with altered and unaltered anodes. The setup included a 3.5 wt% NaCl aqueous solution as the electrolyte and a commercial air electrode with a Pt/C electrocatalyst as the cathode. Pure magnesium samples (Mg) were ground with abrasive papers up to 3000 grit and ultrasonicated in an acetone solution for 15 min before draining. Magnesium electrodes with a surface area of roughly $3 \times 3\,\mathrm{cm}^2$ were immersed in a 3.5 wt% NaCl solution. The discharge performance of Mg-air batteries with coated PANI and noncoated PANI anodes was investigated for 8000 sec. Utilizing galvanostatic discharge, the cell voltage was evaluated at $10\,\mathrm{mA\,cm}^2$ with a commercial air electrode featuring a Pt/C catalyst as the cathode.

3 Results and Discussion

3.1 Electrochemical results

Figure 1a illustrates the Tafel curves of Mg anodes, both with and without a coating. The sample coated with PANI exhibits the lowest corrosion potential, while the uncoated pure Mg sample shows the highest corrosion potential. According to the Tafel polarization analysis (Table 1), the Mg-PANI alloy demonstrates the best performance. The Tafel test results are detailed in Table 1. The Ecorr and Icorr values for

Mg-PANI and Mg are $-1.01\,\mathrm{V}$ and $5.06 \times 10^{-5}\,\mathrm{A/cm^2}$, and $-1.49\,\mathrm{V}$ and $6.3 \times 10^{-4}\,\mathrm{A/cm^2}$, respectively, indicating the lowest corrosion potential. Meanwhile, the uncoated Mg samples displayed the highest corrosion potential. Figure 1b presents the OCP images of Mg, both uncoated and coated with polyaniline, with OCP values of 1.54 V and 1.53 V, respectively. The results obtained before and after applying the PANI coating confirm its effectiveness in enhancing the performance of the anode. Moreover, in coated samples like Mg-PANI (28 mV/dec), the increased anodic slope suggests the coating effectively acts as a barrier, limiting magnesium exposure and slowing its dissolution. Regarding cathodic hydrogen evolution, a higher cathodic slope (39 mV/dec) indicates fewer active sites for hydrogen generation, a result of the synergistic influence of PANI. Functioning as a dual-purpose inhibitor, the PANI coating enhances stability and protection by leveraging its conductivity, structural integrity, and catalytic efficiency.

These analyses demonstrate the superior performance of the coated anode samples compared to the uncoated ones, as further supported by comparisons with other materials reported in the literature (Table 2).

The corrosion potential of Mg, coated and uncoated with PANI, in a 3.5% NaCl solution over 600 seconds at current densities of 10 and $70\,\mathrm{mA/cm^2}$ is presented in Figure 2. The PANI-coated Mg demonstrates superior electrochemical activity, with potentials of $-1.466\,\mathrm{V}$ and $-1.471\,\mathrm{V}$, respectively, compared to pure Mg. The CP tests, following the Tafel and OCP polarization results, confirm the excellent performance of the PANI coating on Mg as an anode electrode. This indicates that the Mg coated with PANI possesses the greatest corrosion protection. The synthesized polymer coating effectively reduces the corrosion of the anode surface, leading to reduced corrosion density for Mg-PANI compared to pure Mg. Surface variations lead to minor fluctuations in the curves due to the integrated contribution of the magnesium metal and the applied coating. Overall, the electrochemical tests demonstrate the effective electrochemical response of the anode electrode following the application of the PANI coating on its surface.

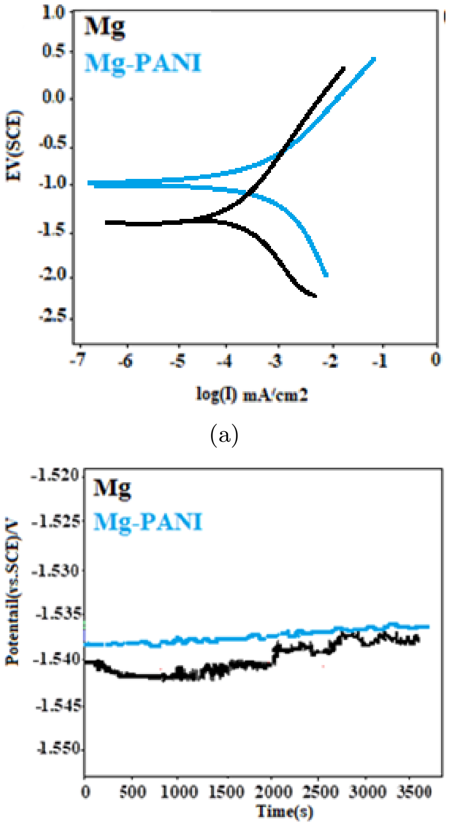

(a)

(b)

Fig. 1. (a) Tafel and (b) OCP curves of bare and Mg-PANI electrodes in a 3.5 wt% NaCl electrolyte.

Table 1. Polarization test results of Mg electrode coated with PANI and without coating.

Sample	E_{corr}, V (SCE)	I_{corr}, $\mathrm{A\,cm^{-2}}$	β_a ($\mathrm{mVdec^{-1}}$)	β_c ($\mathrm{mVdec^{-1}}$)	E_{OCP} (VSCE) (V)
Mg	-1.49	6.3×10^{-4}	28	39	-1.54
Mg-PANI	-1.01	5.06×10^{-5}	36	45	-1.53

Table 2. Comparing the anode performance of various coatings in Mg-air batteries.

Sample	E_{corr}, V (SCE)	I_{corr}, $\mathrm{A\,cm^{-2}}$	β_a ($\mathrm{mVdec^{-1}}$)	β_c ($\mathrm{mVdec^{-1}}$)	E_{OCP} (VSCE)(V)
Mg-PANI	-1.01	5.06×10^{-5}	36	45	This work
Mg	-1.49	6.3×10^{-4}	28	39	This work
Mg/PANI@3D-FCNT	-1.151	0.63×10^{-4}	-	-	36
Ti-implanted AZ31	-1.45	7.827×10^{-5}	-	-	37

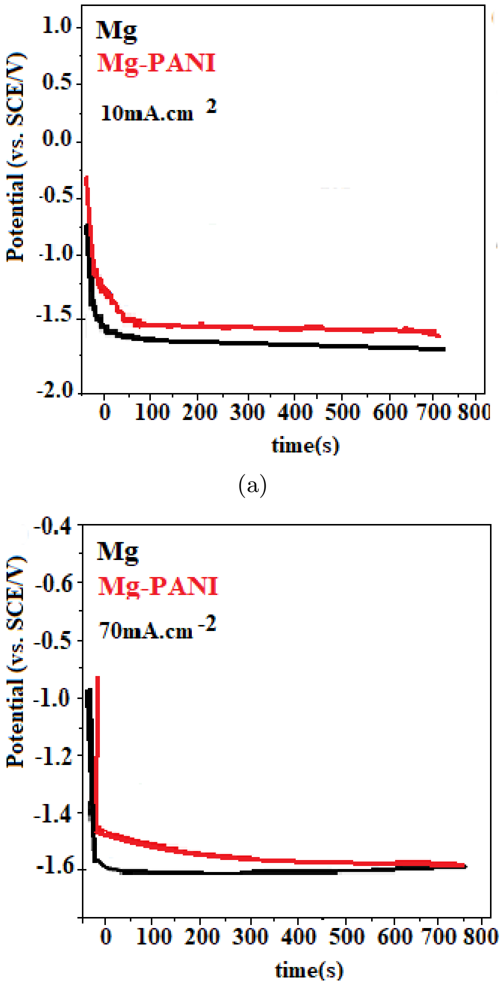

(a)

(b)

Fig. 2. Galvanostatic potential-time curves of the different samples in 3.5% NaCl electrolyte at various current densities. (a) 10 mA/cm^2, **(b)** 70 mA/cm^2.

Figures 1 and 2 display that the PANI-coated Mg stands out with superior corrosion resistance. The synthesized polymer coating effectively reduces corrosion on the anode surface and results in a lower corrosion density in the Mg-PANI compared to pure Mg. The slight fluctuations in the curves can be attributed to surface changes due to the combined action of the coating and Mg metal. Overall, the electrochemical tests confirm the effective electrochemical activity of the anode electrode after applying the PANI coating. Moreover, owing to its reduced density and outstanding mechanical performance compared to pure Mg, Mg coated with PANI has demonstrated excellent corrosion resistance. The performance and durability of the designed coating in mitigating corrosion on the Mg anode surface are illustrated in the impedance diagram. As shown in Figure 3, Mg-PANI exhibits good stability. The resistance of the coated Mg was estimated using impedance measurements in the high-frequency range of the EIS spectrum. By applying frequencies of 100 mHz to 10 kHz, the polarization resistance was calculated from the measured impedance difference, which was subsequently applied to determine the rate of corrosion [35].

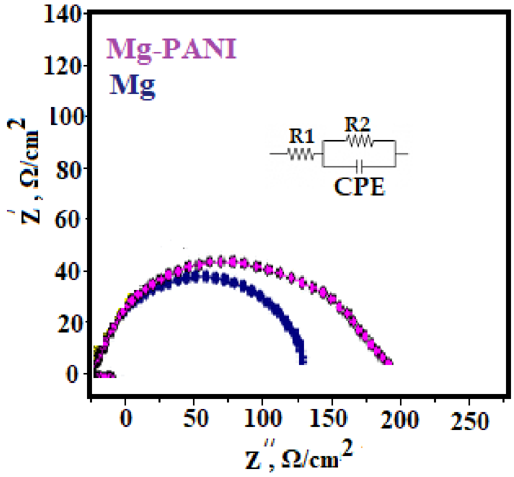

Fig. 3. Nyquist plots of Mg and Mg-PANI coating.

The diameter of the impedance arcs (capacitor rings) directly correlates with the properties of the materials on the anode surface, potentially reducing corrosion and minimizing hydrogen release during the reaction. The charge transfer mechanism at the solution/electrode interface governs the corrosion reaction of the anode. Incomplete semicircles may occur due to frequency dispersion. A reduction in the diameter of these semicircles or the appearance of an additional semicircle indicates coating deterioration. Magnesium surface corrosion is governed by an electrochemical process that takes place when the Mg is in contact with the electrolyte, resulting in the deposition of $Mg(OH)_2$ and the emission of H_2 on the Mg surface [36]. However, PANI coating layers of a specific thickness have a beneficial impact on the corrosion rate of Mg. The designed coating influences the anodic process by dissolving the corrosion products. Consequently, the coating applied to the surfaces of pure Mg significantly reduces the corrosion rate. Overall, the PANI-coated Mg demonstrates the most favorable performance [37].

PANI enhances the corrosion resistance of Mg by acting as both a physical barrier and an electrochemical stabilizer. The protective PANI coating limits direct electrolyte contact with the magnesium surface, reducing unwanted oxidation. Additionally, PANI's redox-active properties help regulate surface charge distribution, minimizing localized corrosion sites. EIS results indicate increased charge transfer resistance (R_t), suggesting that PANI reduces electron exchange at the anode, thus suppressing corrosion. The presence of

PANI also stabilizes surface pH by mitigating excessive alkalization, preventing the formation of an unstable $Mg(OH)_2$ layer. These combined effects contribute to improved discharge efficiency and prolonged anode lifespan in Mg-air batteries. Also, the impedance results of uncoated Mg show an increase in the rate of corrosion and instability of the anode. Therefore, it can be stated that the protective layer applied to the surface of Mg has remarkably reduced the corrosion rate.

Based on the equivalent circuit data in Table 3, the Mg-PANI-coated anode exhibits the highest charge transfer resistance ($189\,\Omega\,cm^2$), underscoring the exceptional protective performance of the coating. The gradual increase in load resistance over time is linked to the progressive formation of the $Mg(OH)_2$ protective layer on the Mg surface. The PANI-coated Mg electrode demonstrates significantly greater resistance to self-corrosion compared to uncoated Mg. Consequently, these materials hold promise for effectively mitigating corrosion and reducing hydrogen release during the reaction. In comparing the pure Mg and the Mg-PANI, the Mg-PANI sample exhibited superior performance as an anode electrode. The improved efficiency of the Mg-PANI, compared to pure Mg, can be attributed to its greater strength and stability [38].

Table 3. Electrochemical equivalent data for Mg-PANI, and bare Mg

Sample	$R1$ ($\Omega\,cm^2$)	R_2 (Ωcm^2)	CPE (F)
Mg	69.1	145	0.235
Mg-PANI	81.6	189	0.621

The values obtained from ICP-OES analysis for bare samples coated with polyaniline in 10 ml of 3.5% NaCl electrolyte after 7 days of immersion are shown in Table 4.

Table 4. Precipitation obtained in the electrolyte by ICP-OES analysis for samples (Mg-PANI and pure magnesium) coated with polyaniline after 7 immersions.

Content(ppm)	Element	Sample	NO
68.22	Mg	Mg	1
39.96	Mg	Mg - PANI	2

By analyzing the 2 samples mentioned in the table, the Mg element was identified in a diverse variety of concentrations with a detection limit of ppm. Table 4 shows the corrosion rate of magnesium according to the magnesium concentration in the electrolyte.

In the comparison of magnesium precipitation in samples 1 and 2 within a 3.5% NaCl electrolyte, sample 1 (magnesium without polyaniline coating) exhibits the highest precipitation at 68.22 ppm. Consequently, the Mg-PANI sample demonstrates less corrosion than the Mg sample. These findings emphasize the beneficial impact of the polyaniline coating on the anode electrode, attributed to the stable properties and characteristics of Mg-PANI compared to pure Mg.

Figure 4 illustrates the discharge performance of Mg-air batteries in a 3.5% NaCl electrolyte, with modifications to the anode electrode surface (Mg with PANI coating and Mg without PANI coating) after 8000 seconds at a constant current of $10\,mA/cm^2$. During electrical power transmission, the anode undergoes oxidation as it interacts with the cathode in ambient air, resulting in an oxidation reaction. According to the time-discharge curve, the voltage of Mg at a current density of $10\,mA/cm^2$ decreased rapidly, with the discharge stopping after approximately 1000 seconds. This sample exhibited two voltage drops. In contrast, no rapid voltage drop was observed in the Mg-PANI at the same current density. After approximately 3000 seconds of discharge, the voltage remained constant at 1400. Thus, Mg-PANI demonstrates a more stable structure and superior performance than pure Mg.

Figure 5 illustrate the surface degradation of Mg-PANI compared to pure Mg after discharging for 8000 seconds at a density of $10\,mA/cm^2$ in a 3.5 wt% NaCl solution, following the removal of by-products of the discharge process. The Mg-PANI anode exhibits relatively regular and uniform discharge holes, whereas the uncovered sample displays larger holes and more cracks. After the discharge test, fewer hydrogen gas bubbles were observed on the Mg electrode with the PANI coating, indicating improved electrochemical performance. The coated electrode developed a smoother and denser surface post-discharge, whereas the uncoated Mg sample exhibited deep cracks following testing. These stability test results confirm that the Mg electrode with the PANI coating demonstrates enhanced stability and performance, providing greater resistance to surface self-corrosion compared to the uncoated sample.

Figure 6 depicts Mg and Mg-PANI after 7 days of immersion in a 3.5% NaCl electrolyte. The uncoated Mg sample exhibits large holes and significant corrosion compared to the Mg-PANI sample. Figure 6(b) shows that Mg-PANI undergoes uniform and regular corrosion, whereas the uncoated Mg sample displays larger and smaller holes. The PANI coating on Mg results in a uniformly corroded surface, a desirable corrosion mode with minimal destructive power. This uniform corrosion is a result of the formation of numerous corrosion cells across the Mg-PANI surface. SEM image comparisons reveal that Mg with PANI coating exhibits improved resistance compared to the uncoated sample. With its thermal and radiation stability and favorable conductivity properties, the PANI coating effectively serves as a corrosion-resistant layer for the Mg anode. PANI exhibits electrochemical activity that helps regulate localized pH changes at the electrode surface. By preventing excessive alkalization, it minimizes the conditions that accelerate the formation of insulating corrosion products, which can degrade battery performance. Furthermore, PANI enhances charge transfer processes, improving the uniformity of ion migration and mitigating irregular corrosion patterns. Its conductive nature aids in facilitating electron movement, allowing for more controlled electrochemical reactions rather than uncontrolled degradation of the magnesium anode. It performs exceptionally well on the Mg-PANI anode electrode material in Mg-air batteries [39].

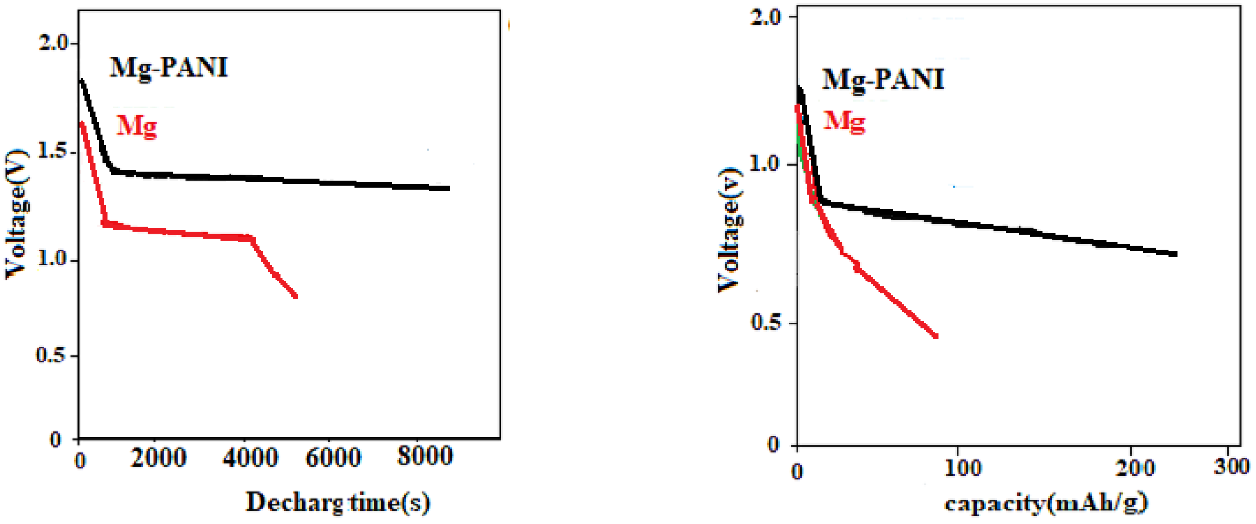

(a) (b)

Fig. 4. (a) Discharge, and (b) the capacity of Mg-PANI and bare Mg anodes.

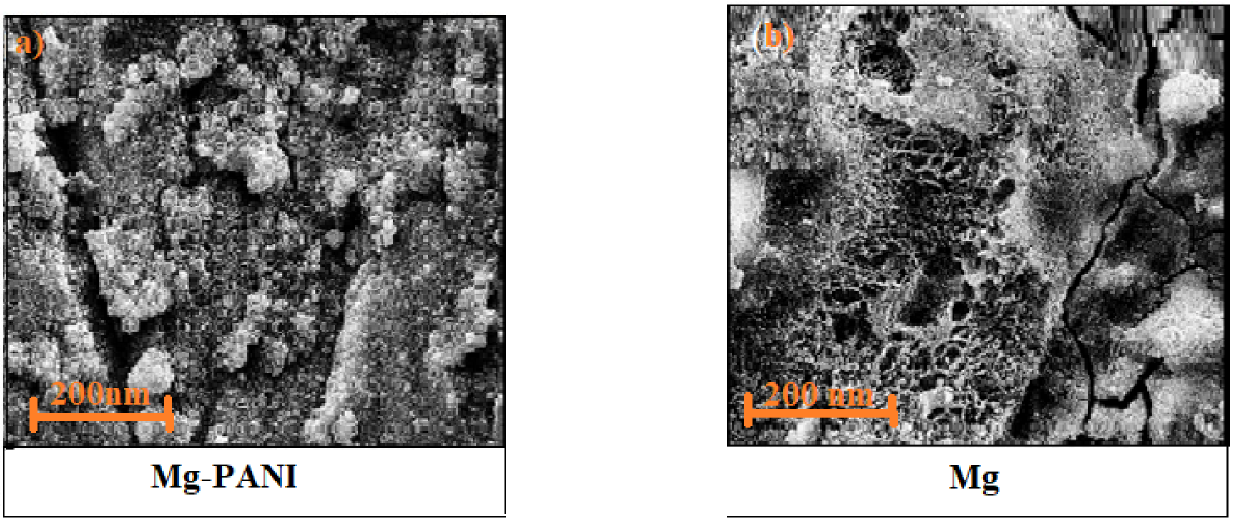

(a) (b)

Fig. 5. (a) Surface morphology of Mg-PANI electrode (b) bare Mg after discharging for 8000 seconds at a density of $10\,\mathrm{mA/cm^2}$ **in a 3.5 wt% NaCl solution.**

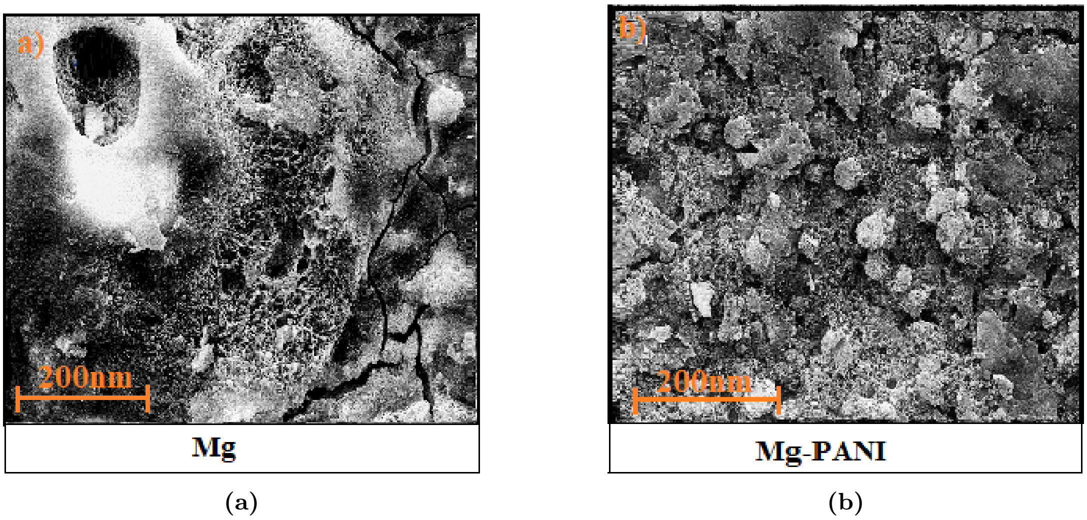

(a) (b)

Fig. 6. The surface morphology of Mg and Mg-PANI after 7 days of immersion in 3.5% NaCl electrolyte.

Figure 7(a) pertains to PANI, displaying three wide and intense diffraction peaks in the range of $2\theta = 20\text{-}30°$, illustrating the structural crystallinity of the synthesized PANI [40–43]. The pattern presented in Figure 7(b) is related to the Mg electrode. The sharp peak between 20° and 27°, highlighting the Mg structure [39, 44, 45].

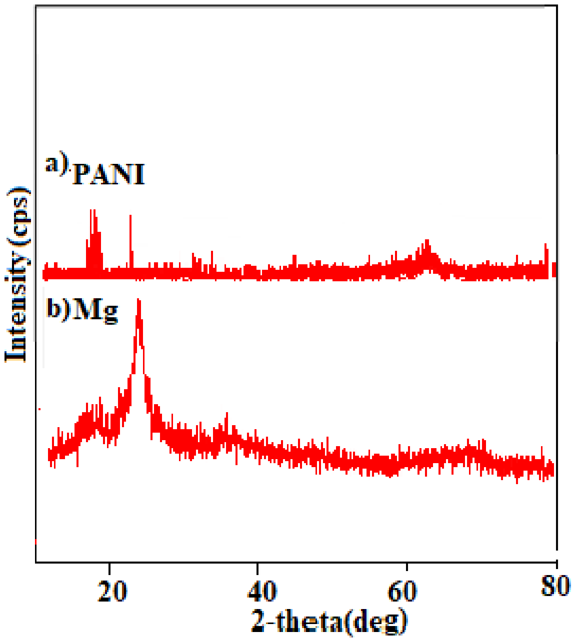

Fig. 7. XRD patterns of Mg and synthesized PANI.

The EDX and mapping results of each element in the coated sample showed that all elements were well scattered over the surface of the Mg sample. In other words, the data clearly shows the presence of all elements.

4 Conclusion

In this study, the discharge behavior of Mg, coated with as-synthesized PANI to modify the anode surface, was evaluated using electrochemical techniques. The performance was probed as anodes in Mg-air batteries in a 3.5 wt% NaCl electrolyte. In all electrochemical tests, Mg-PANI demonstrated improved anode efficiency. During the high current density half-cell test, Mg-PANI exhibited stronger discharge activity with OCPs of 1.53 V than 1.54 V for the Mg sample. These results indicate excellent electrochemical activity. Additionally, the Ecorr and Icorr values for Mg-PANI are $-1.01\,\text{V}$ and 5.06×10^{-5}, respectively, indicating the surface modification of the sample with the lowest potential corrosion. Moreover, the increased capacity of the PANI-coated anode (270 mAh/g), in contrast to the uncoated anode (90 mAh/g), demonstrates the superior effectiveness of the coating in prolonging battery life. Electrochemical analyses, corrosion tests, and battery stability tests confirm the stable performance of the PANI coating in modifying the Mg electrode surface as an anode electrode in Mg-air batteries, effectively controlling anode surface corrosion and enhancing Mg-air battery performance. PANI-coated magnesium anodes improve Mg-air battery efficiency and corrosion resistance, making them viable for portable electronics, marine applications, and emergency power systems. These advancements enhance lightweight energy solutions for the military and transportation sectors, while also enabling seawater-activated batteries for underwater sensors and autonomous marine devices.

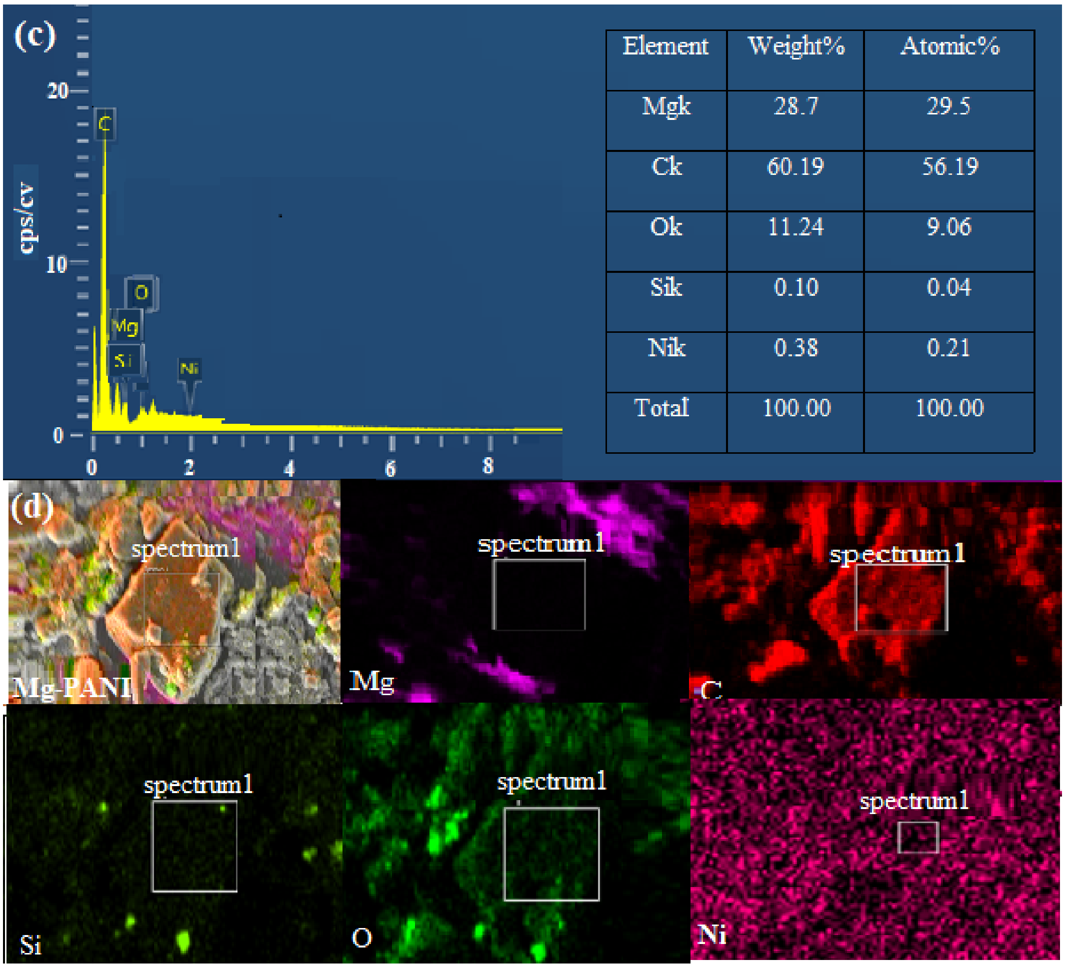

Element	Weight%	Atomic%
Mgk	28.7	29.5
Ck	60.19	56.19
Ok	11.24	9.06
Sik	0.10	0.04
Nik	0.38	0.21
Total	100.00	100.00

Fig. 8. (a,b) indicates the EDX and mapping analysis of Mg-PANI.

Acknowledgments

This study was supported by the Laboratory of Hydrogen and Fuel Cells at Yasouj University.

Conflict of Interest

The authors declare that they have no conflicts of interest.

References

[1] Chen X, Jia Y, Liao Q, Jia W, Le Q, Ning S, et al. The simultaneous application of variable frequency ultrasonic and low frequency electromagnetic fields in semi continuous casting of AZ80 magnesium alloy. Journal of Alloys and Compounds. 2019;774:710-20.

[2] Akbarian P, Kheirmand M, Asadi A. Bimetallic 3D hollow-nanoshell FeCo-oxynitride/N and S co-doped carbon nanotubes as a robust bifunctional oxygen electrocatalyst for rechargeable Zn-air batteries. Journal of Materials Science. 2023;58(21):8889-907.

[3] Cheng F, Chen J. Metal–air batteries: from oxygen reduction electrochemistry to cathode catalysts. Chemical Society Reviews. 2012;41(6):2172-92.

[4] Chen X, Ning F, Hou J, Le Q, Tang Y. Dual-frequency ultrasonic treatment on microstructure and mechanical properties of ZK60 magnesium alloy. Ultrasonics Sonochemistry. 2018;40:433-41.

[5] Akbarian P, Kheirmand M. Metal-organic framework-derived Cu@ Co4N nanoparticles anchored on N-doped carbon nanotubes for efficient

and stable ORR activity. Hydrogen, Fuel Cell & Energy Storage. 2023;10(4):327-37.

[6] Marode RV, Lemma TA, Sallih N, Pedapati SR, Awang M, Hassan A. Research progress in friction stir processing of magnesium alloys and their metal matrix surface composites: evolution in the 21st century. Journal of Magnesium and Alloys. 2024;12(6):2091-146.

[7] Atrens A, Shi Z, Mehreen SU, Johnston S, Song GL, Chen X, et al. Review of Mg alloy corrosion rates. Journal of magnesium and alloys. 2020;8(4):989-98.

[8] Wang N, Wang R, Peng C, Peng B, Feng Y, Hu C. Discharge behaviour of Mg-Al-Pb and Mg-Al-Pb-In alloys as anodes for Mg-air battery. Electrochimica Acta. 2014;149:193-205.

[9] Zhang J, Wei J, Li B, Zhao X, Zhang J. Long-term corrosion protection for magnesium alloy by two-layer self-healing superamphiphobic coatings based on shape memory polymers and attapulgite. Journal of Colloid and Interface Science. 2021;594:836-47.

[10] Du H, Wei Z, Wang H, Zhang E, Zuo L, Du L. Surface microstructure and cell compatibility of calcium silicate and calcium phosphate composite coatings on Mg–Zn–Mn–Ca alloys for biomedical application. Colloids and Surfaces B: Biointerfaces. 2011;83(1):96-102.

[11] Zomorodian A, Garcia M, e Silva TM, Fernandes J, Fernandes MH, Montemor MdF. Biofunctional composite coating architectures based on polycaprolactone and nanohydroxyapatite for controlled corrosion activity and enhanced biocompatibility of magnesium AZ31 alloy. Materials Science and Engineering: C. 2015;48:434-43.

[12] Lin Z, Wang T, Yu X, Sun X, Yang H. Functionalization treatment of micro-arc oxidation coatings on magnesium alloys: A review. Journal of Alloys and Compounds. 2021;879:160453.

[13] Zhang D, Peng F, Liu X. Protection of magnesium alloys: From physical barrier coating to smart self-healing coating. Journal of Alloys and Compounds. 2021;853:157010.

[14] Ghanbari A, Warchomicka F, Sommitsch C, Zamanian A. Investigation of the oxidation mechanism of dopamine functionalization in an AZ31 magnesium alloy for biomedical applications. Coatings. 2019;9(9):584.

[15] Sivapragash M, Kumaradhas P, Vettivel S, Retnam BSJ. Optimization of PVD process parameter for coating AZ91D magnesium alloy by Taguchi grey approach. Journal of magnesium and alloys. 2018;6(2):171-9.

[16] Song M, Zhang T, Niu J, Gao H, Shi Y, Zhang Y, et al. Boosting electrochemical reactivity of tin as an anode for Mg ion batteries through introduction of second phase. Journal of Power Sources. 2020;451:227735.

[17] Xu W, Zhao Y, Wang H, Wang H, Pan F, Xu R, et al. Postsynthetic-Modified PANI/MOF Composites with Tunable Thermoelectric and Photoelectric Properties. Chemistry–A European Journal. 2021;27(15):5011-8.

[18] Liu F, Cao G, Ban J, Lei H, Zhang Y, Shao G, et al. Recent advances based on Mg anodes and their interfacial modulation in Mg batteries. Journal of Magnesium and Alloys. 2022;10(10):2699-716.

[19] Yong H, Wei X, Hu J, Yuan Z, Guo S, Zhao D, et al. Hydrogen storage behavior of Mg-based alloy catalyzed by carbon-cobalt composites. Journal of Magnesium and Alloys. 2021;9(6):1977-88.

[20] Chen X, Zou Q, Le Q, Hou J, Guo R, Wang H, et al. The quasicrystal of Mg–Zn–Y on discharge and electrochemical behaviors as the anode for Mg-air battery. Journal of Power Sources. 2020;451:227807.

[21] Asadi H, Suganthan B, Ghalei S, Handa H, Ramasamy RP. A multifunctional polymeric coating incorporating lawsone with corrosion resistance and antibacterial activity for biomedical Mg alloys. Progress in Organic Coatings. 2021;153:106157.

[22] Bakhsheshi-Rad H, Hamzah E, Ismail A, Sharer Z, Abdul-Kadir M, Daroonparvar M, et al. Synthesis and corrosion behavior of a hybrid bioceramic-biopolymer coating on biodegradable Mg alloy for orthopaedic implants. Journal of Alloys and Compounds. 2015;648:1067-71.

[23] Zomorodian A, Garcia M, e Silva TM, Fernandes J, Fernandes M, Montemor M. Corrosion resistance of a composite polymeric coating applied on biodegradable AZ31 magnesium alloy. Acta Biomaterialia. 2013;9(10):8660-70.

[24] Li LY, Cui LY, Zeng RC, Li SQ, Chen XB, Zheng Y, et al. Advances in functionalized polymer coat-

ings on biodegradable magnesium alloys–A review. Acta biomaterialia. 2018;79:23-36.

[25] Li J, Cao P, Zhang X, Zhang S, He Y. In vitro degradation and cell attachment of a PLGA coated biodegradable Mg–6Zn based alloy. Journal of materials science. 2010;45(22):6038-45.

[26] Li H, Peng F, Wang D, Qiao Y, Xu D, Liu X. Layered double hydroxide/poly-dopamine composite coating with surface heparinization on Mg alloys: improved anticorrosion, endothelialization and hemocompatibility. Biomaterials science. 2018;6(7):1846-58.

[27] Wang B, Xu D, Dong J, Ke W. Effect of corrosion product films on the in vitro degradation behavior of Mg-3% Al-1% Zn (in wt%) alloy in Hank's solution. Journal of materials science & technology. 2018;34(10):1756-64.

[28] Zou YH, Wang J, Cui LY, Zeng RC, Wang QZ, Han QX, et al. Corrosion resistance and antibacterial activity of zinc-loaded montmorillonite coatings on biodegradable magnesium alloy AZ31. Acta biomaterialia. 2019;98:196-214.

[29] Xu HY, Zhang L, Wang YF, Han X. Improved anticorrosive property of waterborne epoxy coating by ultrasonic blending with small amounts of polyaniline. Journal of the Iranian Chemical Society. 2022;19(6):2519-26.

[30] Deng M, Wang L, Höche D, Lamaka SV, Jiang P, Snihirova D, et al. Ca/In micro alloying as a novel strategy to simultaneously enhance power and energy density of primary Mg-air batteries from anode aspect. Journal of Power Sources. 2020;472:228528.

[31] Jia D, Liu F, Yang D, Wang W. Research progress of magnesium anode materials and their applications in chemical power sources. International Journal of Electrochemical Science. 2020;15(10):10584-615.

[32] Xue S, Li B, Mu P, Li J. Designing attapulgite-based self-healing superhydrophobic coatings for efficient corrosion protection of magnesium alloys. Progress in Organic Coatings. 2022;170:106966.

[33] Yang Y, Xiong X, Chen J, Peng X, Chen D, Pan F. Research advances in magnesium and magnesium alloys worldwide in 2020. Journal of Magnesium and Alloys. 2021;9(3):705-47.

[34] Iqbal MZ, Faisal MM, Ali SR, Afzal AM, Karim MRA, Kamran MA, et al. Strontium phosphide-polyaniline composites for high performance supercapattery devices. Ceramics International. 2020;46(8):10203-14.

[35] Saranya K, Kalaiyarasan M, Chatterjee S, Rajendran N. Dynamic electrochemical impedance study of fluoride conversion coating on AZ31 magnesium alloy to improve bio-adaptability for orthopedic application. Materials and Corrosion. 2019;70(4):698-710.

[36] Shuai C, Wang B, Yang Y, Peng S, Gao C. 3D honeycomb nanostructure-encapsulated magnesium alloys with superior corrosion resistance and mechanical properties. Composites Part B: Engineering. 2019;162:611-20.

[37] Srinivasan A, Ranjani P, Rajendran N. Electrochemical polymerization of pyrrole over AZ31 Mg alloy for biomedical applications. Electrochimica Acta. 2013;88:310-21.

[38] Álvarez-López M, Pereda MD, Del Valle J, Fernandez-Lorenzo M, Garcia-Alonso M, Ruano OA, et al. Corrosion behaviour of AZ31 magnesium alloy with different grain sizes in simulated biological fluids. Acta biomaterialia. 2010;6(5):1763-71.

[39] Sanches E, Soares J, Mafud A, Fernandes E, Leite F, Mascarenhas YP. Structural characterization of Chloride Salt of conducting polyaniline obtained by XRD, SAXD, SAXS and SEM. Journal of Molecular Structure. 2013;1036:121-6.

[40] Zhao X, Wei J, Li B, Li S, Tian N, Jing L, et al. A self-healing superamphiphobic coating for efficient corrosion protection of magnesium alloy. Journal of colloid and interface science. 2020;575:140-9.

[41] Iqbal MZ, Faisal MM, Sulman M, Ali SR, Afzal AM, Kamran MA, et al. Capacitive and diffusive contribution in strontium phosphide-polyaniline based supercapattery. Journal of Energy Storage. 2020;29:101324.

[42] Mao S, Zhang D, Zhang Y, Yang J, Zheng J. A universal coating strategy for controllable functionalized polymer surfaces. Advanced Functional Materials. 2020;30(40):2004633.

[43] Iqbal MZ, Alam S, Afzal AM, Iqbal MJ, Yaqoob K, Kamran MA, et al. Binary composites of strontium oxide/polyaniline for high performance supercapattery devices. Solid State Ionics. 2020;347:115276.

[44] Ramezanzadeh B, Moghadam MM, Shohani N, Mahdavian M. Effects of highly crystalline and conductive polyaniline/graphene oxide composites on the corrosion protection performance of a zinc-rich epoxy coating. Chemical Engineering Journal. 2017;320:363-75.

[45] Feliu Jr S, Samaniego A, Bermudez EA, El-Hadad AA, Llorente I, Galván JC. Effect of native oxide film on commercial magnesium alloys substrates and carbonate conversion coating growth and corrosion resistance. Materials. 2014;7(4):2534-60.